УДК 539.12...16

FLUCTUATIONS AND CORRELATIONS IN LONGITUDINAL DEVELOPMENT OF ELECTROMAGNETIC SHOWERS PRODUCED BY GAMMA QUANTA BETWEEN 200 AND 3500 MeV

B.Słowiński

The longitudinal development of electromagnetic showers created by photons of 200-3500 MeV has been studied using the pictures of the 180 liter xenon bubble chamber of ITEP (Moscow). It is found that the longitudinal profile of ionization loss in showers scaled in the average shower depth $\bar{t}$ is independent of the primary photon energy E_γ when $E_\gamma \gtrsim 500$ MeV and $t \gtrsim 0.15\bar{t}$. The conclusion is made about normal distribution of the shower depth t at which, on the average, some part $\bar{A}$ of shower ionization loss is released. Our analysis suggests also the existence of short-range correlation in observation function of individual events of a shower which could be used in order to increase the precision of measurements of the photon's energy.

The investigation has been performed at the Laboratory of High Energies, JINR and at the Institute of Physics of the Warsaw University of Technology.

Флуктуации и корреляции в продольном развитии электронно-фотонных ливней, создаваемых гамма-квантами с энергией от 200 до 3500 МэВ

Б.Словинский

Проведено исследование продольного развития электронно-фотонных ливней, создаваемых фотонами с энергией 200-3500 МэВ. Исходным экспериментальным материалом были снимки 180-литровой ксеноновой пузырьковой камеры ИТЭФ (Москва). Показано, что продольное распределение ионизационных потерь в ливнях, выраженное через относительную глубину $t/\bar{t}$, где $\bar{t}$ – средняя глубина ливня, не зависит от энергии E_γ первичного фотона при $E_\gamma \gtrsim 500$ МэВ и $t \gtrsim 0.15\bar{t}$. Сделан вывод о нормальном распределении глубины ливня t, на которой, в среднем, выделяется доля $\bar{A}$ ионизационных потерь ливня. Обнаружены также короткодействующие корреляции в продольном распределении ионизационных потерь индивидуальных ливней, которые можно использовать для повышения точности определения энергии высокоэнергетических гамма-квантов.

Работа выполнена в Лаборатории высоких энергий ОИЯИ и в Институте физики Варшавского технического университета.

I. Introduction

The longitudinal deposition of energy in electromagnetic showers created by high energy gamma quanta or electrons in dense media is for years most frequently studied in literature as a basic characteristic of the process. Nevertheless our present knowledge in the subject first of all comes to the energy dependence of average shower's profile and its scaling behaviour. Meanwhile for many practical purposes a reliable information about such important features of longitudinal shower development as its fluctuation and correlations are of great interest at present.

In the work we analyse these problems using the pictures of the 180 liter xenon bubble chamber of the Institute of Experimental and Theorerical Physics (Moscow)[1] exposed to the beam of π^- mesons at 3.5 GeV/c.

II. Method and Material

For all 908 selected events of showers satisfying the appropriate criteria and grouped into 22 intervals of primary photon energy E_γ the summary electron and positron (later: electron) ranges (SER) $\Sigma r_i(t, p \mid E_\gamma)/\Delta t\,\Delta p$ have been measured in the picture plane within the squares of constant area $\Delta t \Delta p$ with the side of $\Delta t = 0.6$ radiation length (rl) along the shower axis and $\Delta p = 0.3$ rl in its transversal direction. Here t and p mean the coordinates of a square, t being measured from the conversion point of a shower initiating photon[2]. As is shown[3] the SER are proportinal to the relevant ionization loss (SIL) of shower electrons to an accuracy of about 3 % at least in the central region containing more than 90% of the total shower ionization loss. In more detail methodical problems were expounded earlier[2]. For the purpose of the present work the SER summed over all p at a given depth t are used.

III. Cumulative Profiles

Figs. 1-6 show the scatter plots of the depth t and the part A of a total SIL at such shower depths at which, on the average, the part $\bar{A} = 0.1, 0.2, \ldots, 0.9$ of the total SIL is released. The plots correspond to six values of primary photon energy E_γ. On five plots ($\bar{A}$, t) the fit of the average data performed by the function

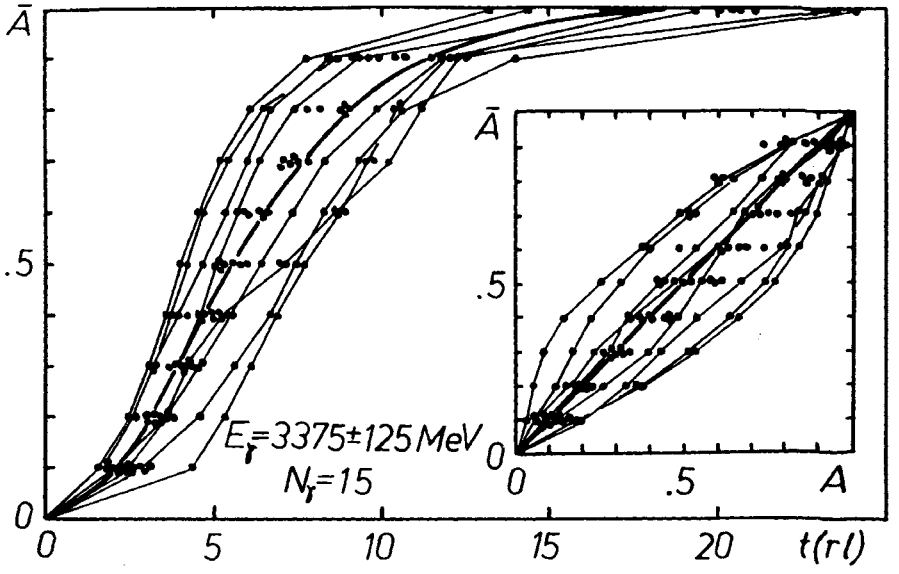

Fig.1. Cumulative longitudinal distribution of ionization loss as a fucntion of the shower depth t and the part A of the ionization loss (inner plot). Bold lines in both plots infer to averaged distributions. The most remote points refering to single shower events are connected by broken lines. N_γ is a number of analysed events of showers produced by photons of energy E_γ = 3375 ± 125 MeV.

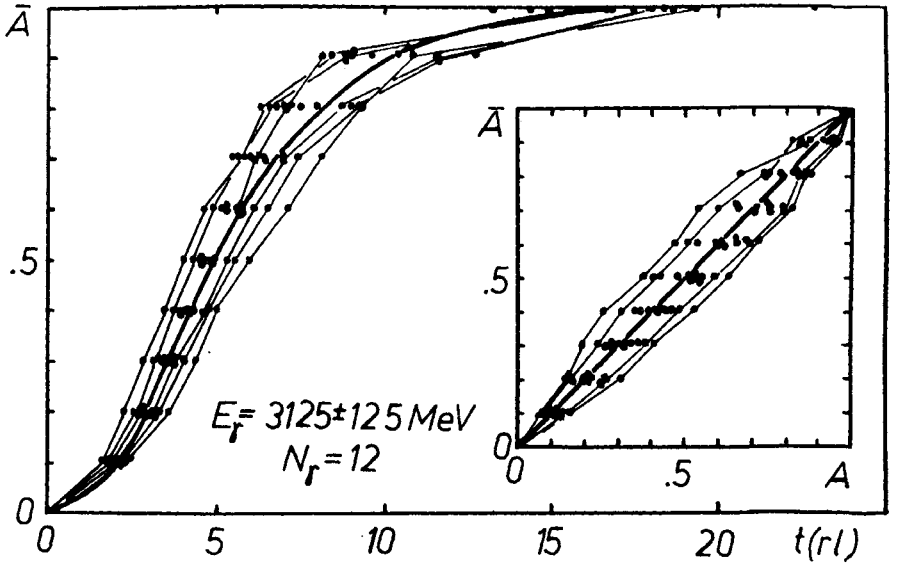

Fig.2. Same as Fig.1 for E_γ = 3125 ± 125 MeV.

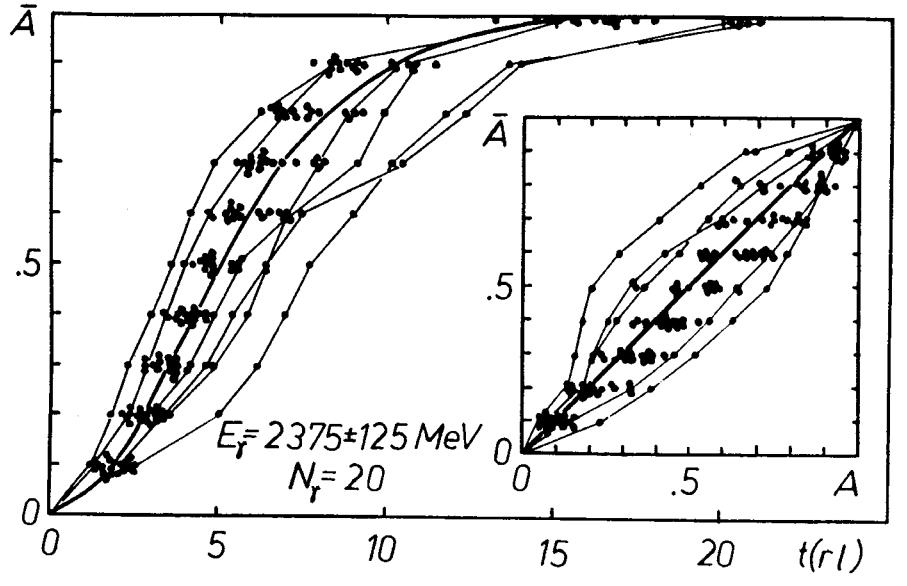

Fig.3. Same as Fig.1 for E_γ = 2375 ± 125 MeV.

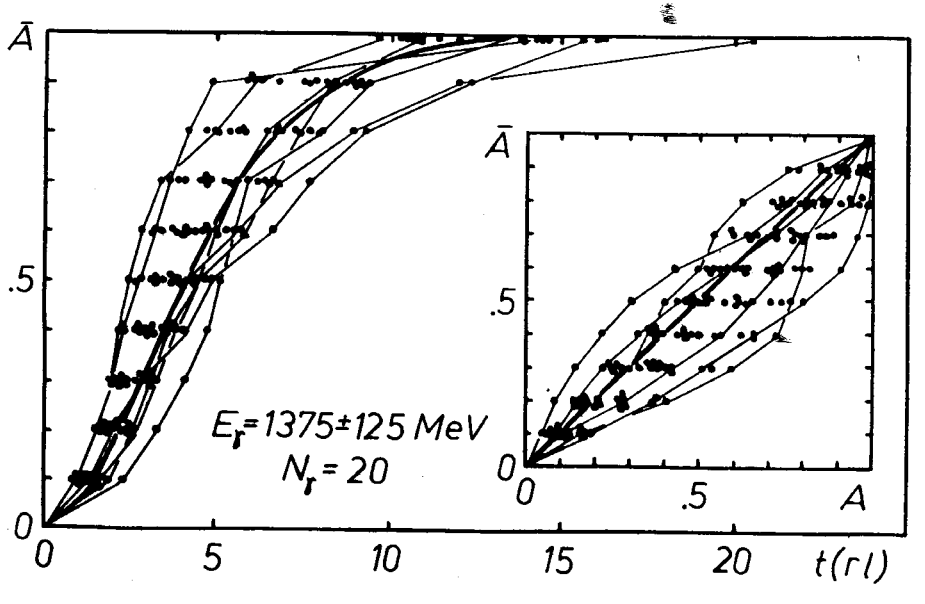

Fig.4. Same as Fig.1 for E_γ = 1375 ± 125 MeV.

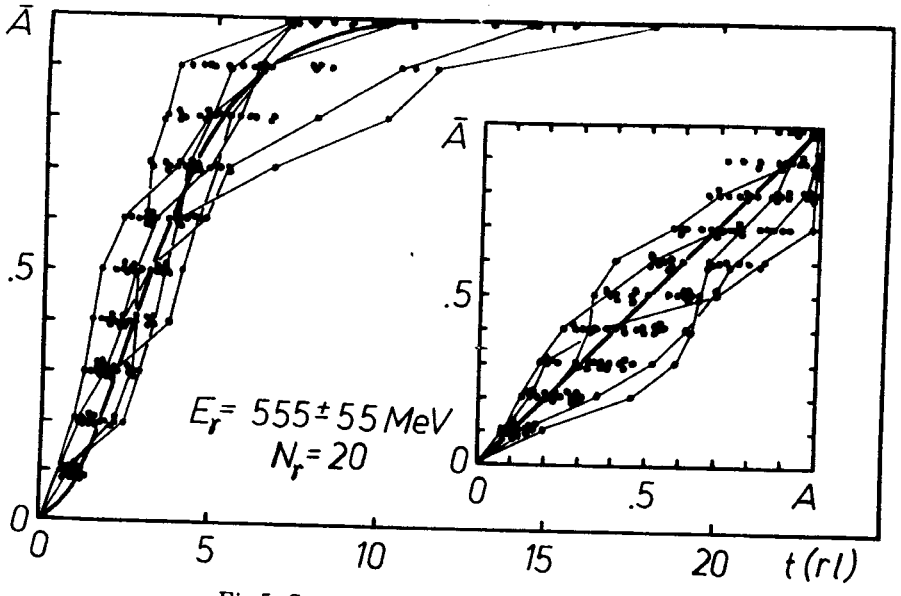

Fig.5. Same as Fig.1 for E_γ = 555 ± 55 MeV.

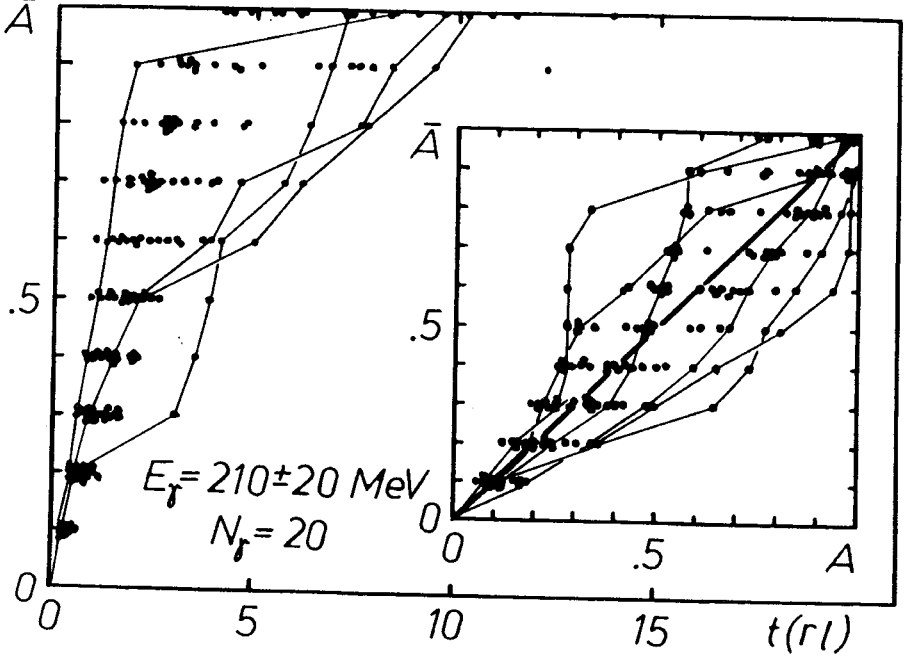

Fig.6. Same as Fig.1 for E_γ = 210 ± 20 MeV.

$$\bar{A}(t) = \int_0^t a_1 x^{a_2} \exp(-x) \cdot dx \qquad (1)$$

valid at $E_\gamma \gtrsim 500$ MeV and $x \gtrsim 0.15$ is superimposed as a smooth line. Here $a_1 = 8.65 \pm 0.34$, $a_2 = 1.65 \pm 0.03$, $a_3 = 2.62 \pm 0.03$, $x = t/\bar{t}(E_\gamma)$,

$$\bar{t}(E_\gamma) = a_t + b_t \cdot \ln E_\gamma, \qquad (2)$$

where $a_t = -4.84 \pm 0.09$ rl, $b_t = 1.32 \pm 0.03$, E_γ is in MeV$^{/4/}$.

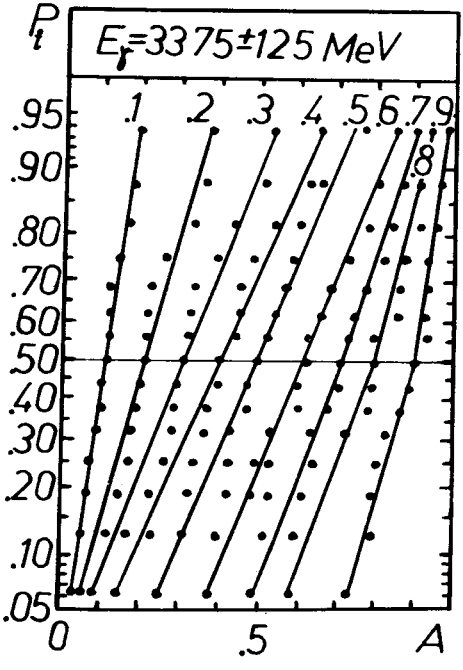

Fig.7. Cumulative distribution of ordered values of a part A (points) of ionization loss deposited at the shower depths at which, on the average, the part $\bar{A} = 0.1$, 0.2, ..., 0.9 of the total shower ionization loss is released. The probability P_i is scaled in such a way that a sample of points having a normal distribution should be arranged along a straight line. The lines are drown by eye and at the top of each one the relevant value of $\bar{A}$ is marked ($E_\gamma = 3375 \pm 125$ MeV).

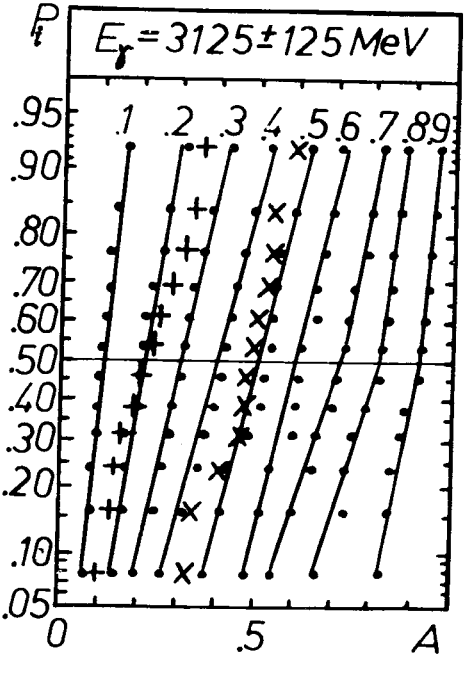

Fig.8. Same as Fig.7 for $E_\gamma = 3125 \pm 125$ MeV. Straight and oblique crosses refer to two different and normally distributed samples of the same size as our experimental data.

1. Fluctuations

We may observe from the figures that both the depth t and the part A are subjected to large fluctuations. Expressed as depending on A, the root-mean-square deviation $\sigma_A^{(t)}$ was parametrized by a simple parabolic function [4]

$$\sigma_A^{(t)} = A\left(\sqrt{\alpha_t^2 + \beta_t(\gamma_t - A)} - \alpha_t\right) \qquad (3)$$

with $\alpha_t = 0.038 \pm 0.001$, $\beta_t = 0.166 \pm 0.005$ and $\gamma_t = 1.01 \pm 0.01$. Moreover, the A values may be considered as following a normal distribution at $\bar{A} < 0.7$ as can be seen from figs.7 and 8 where the probabilities $P_i = i/(N_\gamma + 1)$ for each value of $\bar{A} = 0.1, 0.2, \ldots, 0.9$ at two energies $E_\gamma = 3375 \pm 125$ MeV and 3125 ± 125 MeV are displayed. Here i means a currant number of A ordered according to its increasing value at a given $\bar{A}$ and N_γ is a sample size. The P_i axis is scaled in such a way that the normally distributed data should be arranged along a straight line. For comparison two 12-element's samples selected from a normally distributed population using a table of random numbers [5] are also shown in fig.8. Note also that at $\bar{A} \gtrsim 0.7$ the A-distributions turn out asymmetric because of evident limitation: $A \leq 1$. They can be approximated by two halves of normal distributions with different variances: $\sigma_A(A \lesssim \bar{A}) > \sigma_A(A > \bar{A})$ (figs.7 and 8). The t-distributions, i.e. the

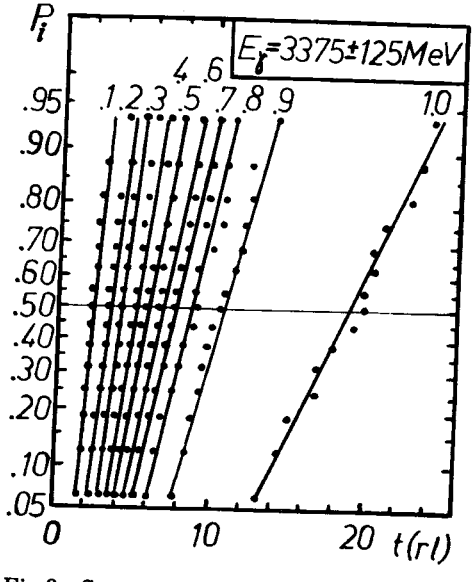

Fig.9. Same as Fig.7 for the shower depth t.

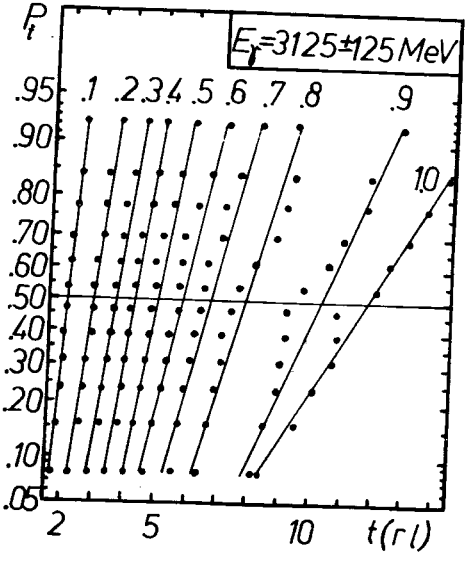

Fig. 10. Same at Fig.7 for the shower depth t and $E_\gamma = 3125 \pm 125$ MeV.

distributions of shower depths at which some fixed part A of SIL is deposited may be also consider as normal ones. Two examples of such distributions are presented in figs.9 and 10 for $E_\gamma = 3375$ MeV and 3125 MeV, respectively, and 9 values of $\bar{A} = 0.1, 0.2, ..., 0.9$ at each E_γ.

2. Correlations

In the $(\bar{A}, t)$-diagrams (figs. 1-6) the most remote points are connected by means of linear segments in such a way that each broken line represents one shower event or, in other words, an observation function. It is to be noted that observation functions become, on the average, more and more smooth with increasing primary photon energy suggesting some increase of short-range correlations. To estimate them quantitatively the slope $X_i = (\Delta\bar{A}/\Delta t)_i$ of an observation function at different t_i has been used when $\Delta\bar{A} = 0.1$ and $\Delta t = t_i - t_{i-1}$, t_i being equal to the shower depth at which, on the average, the part i/10 of the total SIL is deposited (i = 2, 3, ..., 10). Tables 1-6 give the value of the conventionally formulated correlation coefficient [5]

$$r_{ij} = \frac{\mathrm{cov}(X_i, X_j)}{\sigma(X_i)\,\sigma(X_j)} \qquad (4)$$

for six pointed values of energy E_γ (j > i).

Table 1. Value of correlation coefficient r_{ij} defined by (4). $E_\gamma = 3375 \pm 125$ MeV

i \ j	3	4	5	6	7	8	9	10
2	0.52	0.64	0.48	0.42	0.07	0.38	0.02	0.19
3		0.79	0.49	0.42	0.18	0.26	0.41	0.48
4			0.76	0.62	0.33	0.25	0.34	0.27
5				0.90	0.43	0.02	0.13	0.11
6					0.45	0.77	0.26	0.08
7						0.24	0.24	0.22
8							0.14	0.48
9								0.14

Table 2. Same as table 1 for E_γ = 3125 ±125 MeV

i \ j	3	4	5	6	7	8	9	10
2	0.24	0.31	0.05	0.68	0.17	0.17	0.05	0.01
3		0.71	0.67	0.42	0.26	0.39	0.01	0.06
4			0.53	0.01	0.12	0.29	0.17	0.10
5				0.23	0.07	0.04	0.32	0.13
6					0.67	0.68	0.18	0.39
7						0.60	0.48	0.58
8							0.72	0.04
9								0.32

Table 3. Same as table 1 for E_γ = 2375 ±125 MeV

i \ j	3	4	5	6	7	8	9	10
2	0.74	0.03	0.10	0.13	0.18	0.12	0.08	0.29
3		0.24	0.04	0.27	0.19	0.12	0.09	0.08
4			0.53	0.52	0.49	0.53	0.08	0.14
5				0.70	0.61	0.29	0.13	0.06
6					0.76	0.37	0.11	0.02
7						0.56	0.18	0.16
8							0.35	0.16
9								0.09

Table 4. Same as table 1 for E_γ = 1375 ± 125 MeV

i \ j	3	4	5	6	7	8	9	10
2	0.50	0.39	0.08	0.28	0.06	0.03	0.27	0.24
3		0.69	0.50	0.53	0.11	0.11	0.10	0.16
4			0.65	0.56	0.15	0.01	0.12	0.01
5				**0.85**	0.45	**0.22**	**0.37**	0.09
6					0.59	0.26	0.32	0.25
7						0.41	0.38	0.06
8							0.65	0.10
9								0.01

Table 5. Same as table 1 for $E_\gamma = 555 \pm 55$ MeV

i \ j	3	4	5	6	7	8	9	10
2	0.64	0.13	0.08	0.14	0.11	0.10	0.08	0.04
3		0.70	0.26	0.04	0.02	0.08	0.11	0.05
4			0.68	0.20	0.15	0.08	0.01	0.03
5				0.55	0.30	0.23	0.06	0.02
6					0.68	0.44	0.14	0.14
7						0.68	0.25	0.22
8							0.33	0.01
9								0.03

Table 6. Same as table 1 for $E_\gamma = 210 \pm 20$ MeV

i \ j	3	4	5	6	7	8	9	10
2	0.56	0.38	0.30	0.20	0.17	0.15	0.10	0.05
3		0.72	0.59	0.50	0.25	0.21	0.14	0.06
4			0.91	0.68	0.49	0.30	0.22	0.10
5				0.78	0.54	0.36	0.20	0.08
6					0.70	0.41	0.06	0.04
7						0.68	0.09	0.25
8							0.10	0.25
9								0.15

Unfortunately, because of low number of analyzed shower events the quoted results are mainly of qualitative importance. But assuming approximate normality of the slope X_i at a given depth t_i we can infer that there exists a short-range correlation (i.e. $j = i + 1$) essentially within the shower maximum (i.e. at $i = 4 \div 7$) at the level of significance of about 0.01 [6].

IV. Conclusions

The results of the work can be summarized as follows:

1. The average longitudinal profile of showers scaled in $\bar{t}$ is independent both of primary photon energy E_γ and of the material used at $E_\gamma \geq 500$ MeV and $t \geq 0.15\bar{t}$.

2. The shower depths at which some fixed part $\bar{A}$ of the total ionization loss is released are spread approximately normally. Similar property reveals the part A at the depth $\bar{t}$ at which, on the average, the part $\bar{A}$ of the total ionization loss is deposited at a given primary photon energy E_γ. But at $\bar{A} > 0.7$ A-distributions consist of two halves of normal distributions centered at $\bar{A}$ and having different variances so that $\sigma_A(A \lesssim \bar{A}) > \sigma_A(A > \bar{A})$.
3. One can perceive a correlation among two slopes of observation function registered in adjacent absorbent layers mainly within the shower maximum.

References

1. Kuznetsov E.V. et al. — Prib.Tekh.Eksp., 1970, 2, p.56.
2. Słowiński B. — JINR, E1-89-658, Dubna, 1989.
3. Słowiński B., Czyzewska D. — JINR, P13-88-239, Dubna, 1988.
4. Słowiński B. — JINR, E1-90-277, Dubna, 1990.
5. Brandt S. — Statistical and Computational Methods in Data Analysis. North-Holland P.C., 1988.
6. Fisher R.A., Yates F. — Statistical Tables for Biological, Agricultural and Medical Research. Olivier and Boyd, Edinburgh, 1938.

Received on May 24, 1991.